HHS Public Access

Author manuscript

Cancer Discov. Author manuscript; available in PMC 2021 June 01.

Published in final edited form as:

Cancer Discov. 2020 December ; 10(12): 1854–1871. doi:10.1158/2159-8290.CD-20-0312.

Multidimensional analyses of donor memory-like NK cells reveal new associations with response after adoptive immunotherapy for leukemia

Melissa M. Berrien-Elliott[1,#], **Amanda F. Cashen**[1,2], **Celia C. Cubitt**[1], **Carly C. Neal**[1], **Pamela Wong**[1], **Julia A. Wagner**[1], **Mark Foster**[1], **Timothy Schappe**[1], **Sweta Desai**[1], **Ethan McClain**[1], **Michelle Becker-Hapak**[1], **Jennifer A. Foltz**[1], **Matthew L. Cooper**[1], **Natalia Jaeger**[1], **Sridhar Nonavinkere Srivatsan**[1], **Feng Gao**[2], **Rizwan Romee**[1,†], **Camille N. Abboud**[1,2], **Geoffrey L. Uy**[1,2], **Peter Westervelt**[1,2], **Meagan A. Jacoby**[1,2], **Iskra Pusic**[1,2], **Keith E. Stockerl-Goldstein**[1,2], **Mark A. Schroeder**[1,2], **John DiPersio**[1,2], **Todd A. Fehniger**[1,2,#]

[1]Department of Medicine, Division of Oncology, Washington University School of Medicine, Saint Louis, MO, USA.

[2]Siteman Cancer Center, Washington University School of Medicine, Saint Louis, MO, USA.

Abstract

NK cells are an emerging cancer cellular therapy and potent mediators of anti-tumor immunity. Cytokine-induced memory-like (ML) NK cellular therapy is safe and induces remissions in acute myeloid leukemia (AML) patients. However, the dynamic changes in phenotype that occur after NK cell transfer that impact patient outcomes remain unclear. Here, we report comprehensive multidimensional correlates from ML NK cell-treated AML patients using mass cytometry. These data identify a unique in vivo differentiated ML NK cell phenotype distinct from conventional NK cells. Moreover, the inhibitory receptor NKG2A is a dominant, transcriptionally-induced checkpoint important for ML, but not conventional NK cell responses to cancer. The frequency of $CD8\alpha^{+}$ donor NK cells is negatively associated with AML patient outcomes after ML NK cell therapy. Thus, elucidating the multidimensional dynamics of donor ML NK cells in vivo revealed critical factors important for clinical response, and new avenues to enhance NK cell therapeutics.

[#]Correspondence: Melissa M. Berrien-Elliott, Washington University School of Medicine, Campus Box 8007, 660 S. Euclid Ave., St. Louis, MO, 63110, melissa.berrien@wustl.edu, 314-747-1547. Todd A. Fehniger, Washington University School of Medicine, Campus Box 8007, 660 S. Euclid Ave., St. Louis, MO 63110, tfehnige@wustl.edu, 314-747-1385.

[†]Currently address: Dana-Farber Cancer Institute, Harvard University, Boston, MA, USA.

Author contributions: MMBE and TAF conceived and designed the study. MMBE, AFC, CCN., PWong, CCC, JAW., MF, TS, SD, EM, MBH, JAF, SNS, NJ, MLC, and FG collected, analyzed, and assembled the data; RR, JFD, CNA, GLU, PW, MAJ, IP, KS-G, MAS provided clinical care to patients on study; MMBE, AFC, and TAF wrote the manuscript and all authors reviewed the data and edited and approved the final version of the manuscript.

Data and materials availability: The RNA-sequencing data are accessible within Gene Expression Omnibus (GEO) under accession code GSE154694.

Conflicts of Interest: Patents have been filed based on the results of this study. MMBE has received travel funds from MaxCyte and Fludigm and is a consultant for Wugen. GLU has received honorarium from Jazz, Genentech, and Astellas. TAF has served on the scientific advisory boards of Nkarta, Indapta, Gamida Cell, Nektar, and Kiadis Pharma, is a consultant for Wugen, and has received research funding from Affimed, Altor BioSciences, Compass Therapeutics, and HCW Biologics. All other authors have no conflicts of interest to report.

Introduction

Natural killer (NK) cells are cytotoxic innate lymphocytes that are important for mediating anti-viral host defense and responding to malignantly-transformed cells (1). NK cell activation is determined by the balance of signals received through germ-line DNA encoded activating, inhibitory, and cytokine receptors, which differs from T cells that rely on rearrangement of the T cell receptor genes (2). Thus, NK cells are equipped to respond to a variety of malignant cells, and have been investigated as a cellular immunotherapy for acute myeloid leukemia (AML), a clinically challenging blood cancer where the primary curative therapy is hematopoietic cell transplantation (HCT) (3–5).

NK cellular immunotherapies are a nascent, promising, and safe alternative to T cells for cellular cancer immunotherapy (6,7). Several types of NK cell therapy have been shown to mediate anti-tumor responses in patients with AML without cytokine release syndrome (CRS) or immune cell- associated neurotoxicity syndrome (ICANS), which are frequent complications after CAR-T cell immunotherapy approaches (4,5,7–9). However, the in vivo dynamic changes in donor NK cells that occur after transfer have not been extensively investigated, and both donor NK cell-intrinsic and host factors that contribute to treatment response and resistance are poorly understood.

Our group and others have identified memory-like (ML) properties of NK cells after brief activation with the cytokines interleukin (IL)-12, IL-15, and IL-18 followed by differentiation in vitro or in vivo in murine models and NSG mice (5,10–12). In vitro differentiated ML NK cells have increased activating receptors, can ignore the rules of KIR-KIR ligand interactions, exhibit prolonged survival in NSG xenograft models, and have improved effector functions against a wide array of targets (5,13,14). We previously reported the first-in-human clinical trial demonstrating that donor ML NK cells were safe, detectable for several weeks after transfer, and induced complete remissions in high-risk relapsed/refractory (rel/ref) AML patients. However, not all patients responded, and the median duration of response was only a few months (5). The phenotypic changes in ML NK cells that occur during in vivo differentiation, and factors contributing to therapeutic response and resistance, were not explored and remain important questions in the field.

Here, we utilized mass cytometry to understand the dynamic changes that occur in ML NK cells during in vivo differentiation within patients with AML. We discovered that ML NK cells are clearly distinct from conventional and activated NK cells, and have a unique, consistent, well-defined multidimensional signature. This multidimensional analysis was integrated with clinical results and identified NKG2A as the predominant checkpoint on ML NK cells, as well as unexpected characteristics of baseline donor NK cells that predict treatment failure.

Results

Mass cytometry distinguishes in vivo differentiated memory-like NK cells

Our initial report describing the dose-escalation cohort of the first-in-human trial using cytokine (IL-12, IL-15, and IL-18)-induced NK cells to treat patients with rel/ref AML

demonstrated that donor ML NK cells expand and proliferate in vivo in AML patients and result in complete remissions (Fig. 1A) (5). The now complete results of the phase 1 study are described in Supplementary Methods, with ML NK cell therapy being well-tolerated without CRS, graft-versus-host disease (GVHD), or neurotoxicity (Tables S1–S3). Among the 15 evaluable patients, 7 achieved CR (n=3) or CRi (n=4), and 3 achieved a best response of morphologic leukemia free state (MLFS) at day 14 by the IWG response criteria (15), for an overall IWG response rate of 67% and a CR/CRi rate of 47% (Table S1).

Donor NK cells were detected in both patient peripheral blood (PB) and bone marrow (BM) by flow cytometry, with peak expansion occurring 7–14 days post-NK cell infusion for patients at all dose levels (5). We hypothesized that in vivo differentiated ML NK cells are distinct from baseline NK cells and NK cells acutely activated with cytokines. To test this, patient PB and BM were analyzed using a 37 marker NK cell mass cytometry panel (Table S4, Fig. S1A–B) and major immune cell subsets were identified using FlowSOM (16) (Fig. 1B, Fig. S1C), including NK cells. Donor NK cells in recipient PBMC were identified using donor- and recipient-specific HLA monoclonal antibodies (mAbs) (Fig. S1B). Donor NK cells were compared at the time of initial isolation (baseline), following 12–16 hour cytokine activation (immediately prior to infusion), and within patient PB or BM mononuclear cells (when available) 7 days following NK cell infusion using t-SNE-based analysis (viSNE). Based on 25 markers, baseline (BL), cytokine-activated (ACT) and memory-like (ML) NK cells are distinct (Fig. 1C–D, Table S4) as indicated by discrete islands within the viSNE maps. These distinctions are consistent across the 11 available patients assessed by mass cytometry at this time point (Table S1, Fig. 1E, $p > 0.001$ as determined by 2-way ANOVA, see methods). For a majority of the patients, donor NK cells are the main lymphocyte subset by frequency and total numbers (Fig. 1F–G), confirming initial flow cytometry results on a subset of patients (5). Within the dose level 3 cohort (2–10e^6 ML NK cells/kg), a significant association between NK cell frequency or absolute cell numbers in PB at day 7 and clinical response was not detected, although this study was not powered for this correlative endpoint (Fig. S1D). Similarly, we did not detect an association between T_{reg} cell numbers or frequency and patient responses, different from other types of NK cell therapy (17). Total circulating $CD34^+$ cells (expressed on most AML) were significantly negatively associated with response, as expected (Fig. S1D).

In vivo differentiated memory-like NK cells are phenotypically distinct

Based on in vitro studies, we hypothesized that ML NK cells could be distinguishable from conventional NK cells by examining a large number of cell surface and intracellular markers. Using the median expression of markers for each BL, ACT, and ML NK cell subset defined based on t-SNE analysis (Fig. 1), we identified the markers significantly associated with each NK cell type. ACT NK cells were defined by significantly decreased CD56 and increased CD25, CD69, and CD137, which are well-defined markers of acute NK cell activation, and consistent with our in vitro reports (Fig. 2A–B Fig. S2A–B) (5,13). ML NK cells were defined by significantly increased CD56, Ki-67, NKG2A, and activating receptors NKG2D, NKp30, and NKp44 (Fig. 2A–B, Fig. S2A). Additionally, modest decreases in the median expression of CD16 and CD11b were observed (Fig. 2A–B). ML NK cells expressed CD16 following in vivo differentiation (median percent positive 69 +/− 16%), consistent

with prior studies demonstrating ML NK cells have enhanced antibody-dependent cellular cytotoxicity (14). Increased frequency of TRAIL, CD69, CD62L, NKG2A, NKp30 positive NK cells were observed in ML NK cells compared to both ACT and BL, while the frequencies of $CD27^+$ and $CD127^+$ NK cells were reduced (Fig. S2C). Finally, unlike in vitro differentiated ML NK cells, in vivo differentiated ML NK cells did not express CD25 (IL-2Rα) (Fig. 2A–B, Fig. S2C) (5). We postulate this may be due to in vivo ligation by low dose IL-2 used to support ML NK cells.

In one case, a CMV seropositive donor's NK cells were predominately $CD57^+NKG2C^+$, which are presumably comprising adaptive NK cells (18,19). Using mass cytometry, we were able to determine that adaptive NK cells could also differentiate into ML NK cells in vivo, as the cells exhibited a ML NK cell signature, including increased CD56 and activating receptor expression (CIML020, Fig. S2B, Fig. S3A–B). However, the fraction of $CD57^+NKG2C^+$ cells remained constant at BL, ACT, and following in vivo ML NK cell differentiation, suggesting that the presence of adaptive markers and biology did not impact ML NK cell differentiation. NKG2C expression was modest on the remaining donor NK cells and was not altered by in vivo ML NK cell differentiation (Fig. S2C).

Because this patient had sufficient donor and recipient NK cells for advanced analysis, PB NK cells at D7 were examined (Fig. S3C–E). Using the same analysis approach (Fig. 2A–B), donor and recipient NK cells were compared using viSNE, and represent distinct populations (Fig. S3C–E). The separation of these populations is confirmed by HLA-A2 staining (Fig. S3D). Finally, the donor ML NK cells demonstrate the consistent ML phenotype, whereas the recipient NK cells do not have increased NKG2A, are $CD11b^+$, and have lower activating receptor expression compared to donor ML NK cells (Fig. S3E). These analyses were not possible for additional patients due to a paucity of recipient NK cells present at D7, but support that ML NK cells are phenotypically distinct from baseline NK cells.

Memory-like NK cells are similar between patient bone marrow and blood

Since AML routinely involves the BM as a unique AML microenvironment, patient bone marrow mononuclear cells (BMMC) were also examined and compared to PB ML NK cells using mass cytometry at day 7 or 8 post-infusion. Consistent with our previous report, donor NK cells trafficked to the BM and represented the major population observed in this tissue, for most patients assessed (Fig. 3A, Table S4) (5). Using t-SNE analysis (Fig. 1–2), PB and BM donor NK cells had a similar multidimensional phenotype when compared to each other, but were again distinct from BL NK cells (Fig. 3B–C). Although median expression of most markers assessed was similar between BM and PB NK cells, BM $donor^+$ NK cells were significantly reduced in NKp46 (PB 18.66 ± 2.14 SEM v BM 7.66 ± 2.56, $p = 0.006$), potentially indicating down-regulation after interaction with AML blasts. KIR expression and KIR diversity on in vitro differentiated ML NK cells did not vary (5). In order to understand how KIR repertoire was altered by in vivo donor ML differentiation, we compared KIR diversity on donor BL and in vivo differentiated ML NK cells (5,20). If a particular subset of KIR-expressing cells had a proliferative advantage in vivo, we would

expect KIR diversity to decrease. However, here we see KIR diversity modestly increased, without significant changes in any single KIR (Fig. S4A–B).

Donor memory-like NK cells differentiated in patients are polyfunctional ex vivo

For a subset of patients with adequate cell numbers, ex vivo functional responses against K562 leukemia targets were examined using mass cytometry. Freshly isolated PBMC were co-incubated with K562 cells for 6 hours; degranulation (CD107a), cytokine production (IFN-γ, TNF) and chemokine production (MIP-1α) were measured using the functional mass cytometry panel (Fig. 4A, Table S4). When co-cultured with leukemia targets, donor ML NK cells produced significantly increased IFN-γ and MIP-1α, compared to unstimulated NK cells (Fig. 4B). When we assessed polyfunctional responses, we observed 46–99% of donor NK cells are producing at least 1 cytokine/chemokine in response to tumor triggering (Fig. 4C). Previous work reported that ML differentiation improved effector functions of unlicensed NK cells (14). In order to investigate if in vivo ML differentiation impacts unlicensed NK cell functionality, we examined the effector functions of single KIR^+ donor NK cells in response to K562. NK cells that were unlicensed in the donor would be expected to produce less effector molecules compared to licensed NK cells. In most cases, the unlicensed KIR-expressing ML NK cell subsets produced IFN-γ, TNF, MIP-1α and express CD107a similarly to the licensed KIR-expressing ML NK cell subsets (Fig. 4D), consistent with the idea that unlicensed donor ML NK cells have enhanced function following ML differentiation in vivo. However, interpreting these in vivo data is complicated by the fact that each KIR is predicted to be licensed in the patient (Fig. 4D), leaving open the possibility that a licensing event also occurred after in vivo transfer.

NKG2A is a dominant inhibitory checkpoint on memory-like NK cells

In order to determine if any markers were associated with treatment failure (TF), we assessed the evaluable dose level 3 patients with available CyTOF data [3 TF, 5 responders (R)] using Citrus (21). Citrus identified that NKG2A median expression on donor ML NK cells in the PB at D7 was significantly associated with TF (SAM, FDR < 0.01). Indeed, NKG2A median expression was significantly increased on donor NK cells transferred into patients with subsequent TF compared to those who achieved an IWG response (Fig. 5A–B). In contrast, NKG2A expression on baseline donor NK cells in this study was 8–76% with a median of 38% expression (Fig. S2C), and was not associated with clinical outcomes. NKG2A is an inhibitory receptor that interacts with the non-classical MHC-I molecule HLA-E (22,23). In order to determine if NKG2A inhibits ML NK cell responses, control or ML NK cells from normal donor PBMC were generated in vitro (Fig. S5A) and stimulated with $HLA\text{-}E^{lo}$ or $HLA\text{-}E^+$ primary AML, and analyzed for IFN-γ production (Fig. S5B–C). ML NK cells responding to $HLA\text{-}E^+$ primary AML produce less IFN-γ on a per-cell basis than ML NK cells triggered with $HLA\text{-}E^{lo}$ tumor targets, consistent with the in vivo association with TF. Next, K562 were generated that overexpress HLA-E to trigger control or ML NK cells (Fig. 5C–D). In these assays, ML NK cells produced more IFN-γ than control NK cells in response to K562, as expected. However, ML NK cells, but not control NK cells, demonstrated reduced IFN-γ production when stimulated with $HLA\text{-}E^+$ K562 targets, compared to HLA-E-negative targets (Fig. 5D). Indeed, the enhanced functionality typically observed in ML NK cells was completely abrogated when HLA-E was present on

the targets (Fig. 5D). In order to determine if NKG2A interactions with HLA-E also inhibited target killing, ML NK cells were incubated with HLA-E^+ or HLA-E^- K562 targets and specific killing was measured in a flow-based killing assay (13). ML NK cells demonstrated a significantly reduced ability to kill HLA-E^+ K562 targets compared to HLA-E^- K562 (Fig. 5E).

Patient BM samples obtained prior to treatment on study were examined by mass cytometry and unbiased FlowSOM was used to define cell populations within the tumor microenvironment (Fig. S6A, Table S4). Using this approach, HLA-E expression on these subsets was compared between responders and TF (Fig. S6B–D). While HLA-E expression on AML blasts was not associated with clinical outcomes, treatment failure was associated with increased HLA-E expression on mononuclear cells within the bone marrow (Fig. S6B–D). These data suggest that increased NKG2A expression and HLA-E expression in the bone marrow, negatively impacted ML NK cell responses in vivo.

NKG2A is transcriptionally induced in ML NK cells

In order to understand the mechanisms underlying this increased NKG2A expression by ML NK cells, qRT-PCR was performed for *KLRC1* (the gene that encodes NKG2A) on in vitro control or differentiated ML NK cells over time (Fig. 5F). ML NK cell, but not control treated NK cells, induced *KLRC1* mRNA. In order to determine if NKG2A expression was occurring de novo, we sorted $CD56^{dim}$ $CD16^+$ $NKG2A^+$ and $NKG2A^-$ cells and examined NKG2A and Ki-67 expression on control and ML NK cells after 7 days in vitro (Fig. 5G). Here, NKG2A negative cells induce NKG2A expression after ML NK cell differentiation, but not control incubation. Additionally, Ki-67 is increased in both $NKG2A^+$ and $NKG2A^-$ NK ML NK cell subsets, but to a greater extent in $NKG2A^+$ ML NK cells (Fig. 5G). These data suggest both an expansion of $NKG2A^+$ NK cells and de novo NKG2A upregulation are responsible for increased NKG2A during ML NK cell differentiation. Previous reports have implicated GATA-3 as a transcription factor that regulates NKG2A expression (24). Indeed, the frequency of GATA-3^+ NK cells is specifically increased in ML NK cells, compared to control NK cells (Fig. 5H). In addition to GATA-3, the transcription factor Eomes was increased in ML NK cells compared to control (Fig. 5I). Further, Eomes and GATA-3 co-expression corresponded with the $NKG2A^{hi}$ cells, suggesting these transcription factors are important for the NKG2A upregulation within ML NK cells (Fig. 5J). Finally, GATA-3 and Eomes are increased in both $CD56^{bright}$ and $CD56^{dim}$ subsets in response to ML differentiation (Fig. S7A–B). GSEA analysis comparing expressed genes in control and ML NK cells revealed ML NK cells were significantly enriched in GATA-3 target genes, compared to control NK cells (Fig. S7C). In similar assays, E4BP4, TCF7, T-bet, Blimp-1, Runx2 and Runx3 median expression were similar between control and ML NK cells (Fig. S7D–E). *BACH2* mRNA expression was also similar between control and ML NK cells (Fig. S7F). Together these data support our previous studies that $CD56^{bright}$ and $CD56^{dim}$ NK cells both have the ability to differentiate in to ML NK cells and demonstrate GATA-3 and Eomes as specifically regulated by ML NK cell differentiation (5,10).

Eomes regulates GATA-3 and promotes ML NK cell enhanced responses to leukemia targets

Since Eomes has a well-defined role in promoting T cell memory (25), we hypothesized that it would be involved in memory formation in cytokine activated NK cells. We used Crispr/CAS9 to delete *EOMES* prior to ML differentiation (Fig. 5K–O). Eomes was reduced in ΔEomes ML NK cells compared to WT control and WT ML NK Cells (Fig 5L–M). The increase in GATA-3 frequency during ML NK cell differentiation was abrogated by loss of Eomes (Fig. 5L–M). Finally, increased IFN-γ responses by ML NK cells compared to control NK cells was also partially abrogated by Eomes deletion (Fig. 5N–O), implicating Eomes as a critical transcription factor for ML NK cell differentiation.

NKG2A checkpoint blockade or elimination restores ML NK cell responses to AML

Since NKG2A interactions with HLA-E are inhibitory for ML NK cells, we hypothesized that abrogating this interaction would restore anti-leukemia responses (Fig. 6). Indeed, ML NK cell IFN-γ production in response to HLA-E^+ K562 was significantly increased by blocking with anti-NKG2A mAb (Fig. 6A–B), returning to similar levels as ML NK cells triggered with K562. HLA−E^+ K562 killing by ML NK cells was also significantly increased in the presence of NKG2A checkpoint blockade, compared to isotype mAb (Fig. 6C). NKG2A checkpoint blockade also enhanced ML NK cell responses, but not control NK cell responses, to multiple primary AML (Fig. 6D–E). To provide an orthogonal loss-of-function approach, we also used CRISPR/Cas9 to disrupt the NKG2A-encoding gene *KLRC1* prior to control or ML NK cell differentiation (Fig. 6F–J). After electroporation with *KLRC1*-targeting gRNA and Cas9 mRNA, cells were rested in vitro for 24 hours and then control (IL-15) treated or ML-cytokine (IL-12, IL-15, and IL-18) activated. Cells were allowed to differentiate for 4–7 days in IL-15, and NKG2A expression was assessed by flow cytometry. Using this approach, NKG2A expression on both control and ML NK cells was significantly reduced (Fig. 6G–H). Wild-type (WT) or ΔNKG2A control or ML NK cells were stimulated with HLA-E^- K562 or HLA-E^+ K562 and IFN-γ measured by flow cytometry. Control NK cell responses were similar in response to K562 with or without HLA-E expression (Fig. 6J), whereas ML NK cell IFN-γ responses were reduced when triggered with HLA-E^+ K562 (Fig. 6J). NKG2A deletion did not impact the enhanced ML NK cell responses to K562 (HLA-E^-), with WT and ΔNKG2A ML NK cells producing similar levels of IFN-γ as expected. However, ΔNKG2A ML NK cell responses were significantly increased compared to WT ML NK cell responses against HLA-E^+ K562 (Fig. 6J). To determine if NKG2C interactions with HLA-E were driving this enhanced response, ΔNKG2A ML NK cells were stimulated with HLA-E^+ K562 in the presence of α-NKG2C blocking antibody, or isotype control (Fig. S8). Blocking NKG2C on WT or ΔNKG2A ML NK cells had no impact on IFN-γ production in response to HLA-E^+ K562 leukemia targets. Overall, these data reveal that NKG2A is a critical inhibitor of ML NK cell responses, but not control NK cell responses, to AML targets.

CD8$^+$NKG2A$^+$ NK cells predict treatment failure and CD8$^+$ NK cells do not proliferate in response to IL-12, IL-15, and IL-18

In addition to NKG2A, Citrus unexpectedly identified that CD8α expression on D7 in vivo differentiated ML NK cell was negatively associated with treatment outcomes (SAM, FDR < 0.01). No other markers were associated by Citrus with clinical outcomes. While there was not a significant difference in CD8$^+$ ML NK cells in vivo at day 7 (TF: Mean 1322 cells/mL ± 1158 cells/mL SD; R: Mean 618.9 cells/mL ± 701.3 cells/mL SD; Unpaired t test p = 0.31), median CD8α expression was significantly increased on donor NK cells in the TF patients compared to the responding patients (Fig. 7A–B). Individually, NKG2A or CD8α expression at BL was not associated with clinical responses. In order to determine if NKG2A and CD8 co-expression at BL was associated with patient outcomes, we examined the frequency of NKG2A$^+$CD8$^+$ NK cells in purified NK cell products (Fig. 7C–E). The frequency of NKG2A$^+$CD8$^+$ NK cells in the product was significantly associated with response to treatment (Fig. 7D–E), with increased frequencies of NKG2A$^+$CD8$^+$ NK cells occurring with treatment failure. Consistent with another study (26), CD8α is expressed on ~ 23% of CD56^{bright} and ~ 35% on CD56^{Dim} NK cells with a high inter-individual variability (Fig. S9A–B). CD8 was not specifically induced in vivo in response to ML NK cell differentiation (Fig. S2C), but was increased in vitro, in both control and ML NK cells. This implicates IL-15 signaling in regulating CD8 upregulation in vitro (Fig. S9C). The majority of CD8$^+$ NK cells are CD8αα$^+$, with a minor subset expressing CD8αβ (Fig. S9D). ML differentiation does not alter these frequencies, relative to control or baseline (Fig. S9E). Finally, CD8$^+$ NK cells do not express CD3, or other T cell receptors (TCR) and represent a subpopulation of NK cells, which distinct from T cells, including iNKT cells (Fig. S9F–G).

To explain the negative association of CD8 with patient outcomes, we hypothesized that CD8α$^+$ NK cells were not optimally responding to IL-12, IL-15, and IL-18 activation. To test signaling competency, freshly isolated NK cells were stimulated with IL-12, IL-15, and IL-18 for 0–120 minutes and phosphorylation of proximal cytokine signaling molecules STAT-4, ERK, STAT-5, p38, and p65 was measured (27,28). For both CD8α$^+$ and CD8α$^-$ NK cells, similar phosphorylation was observed relative to the unstimulated condition (p > 0.05; One sample t test, test value = 1; Fig. 7F). No differences in cytokine receptor signaling were observed between CD8$^+$ and CD8$^-$ NK cells (Fig. 7F). Next, we compared the ability of CD8α$^+$ and CD8α$^-$ NK cells to proliferate in response to ML-cytokine activation. Sorted CD8α$^+$ and CD8α$^-$ NK cells were cell trace violet (CTV)-labeled, activated with IL-12, IL-15, and IL-18, washed after 16 hours, and allowed to differentiate. Proliferation was assessed after 6 days. CD8α$^+$ NK cells divided less compared to CD8$^-$ NK cells, and expression of Ki-67 was reduced, both indicating significantly inferior proliferation (Fig. 7G–H). We hypothesized that the larger number of CD8α$^+$ donor NK cells infused into TF patients were not expanding to the same extent as the predominantly CD8α$^-$ donor NK cells in responding patients. Consistent with this, the amount of Ki-67 in donor NK cells was significantly associated with treatment outcomes (Fig. 7I). However, median Ki-67 expression between NKG2A$^+$ and NKG2A$^-$ ML NK cells in TF and Responders was not significantly different (Fig. S10A–B). Patients with donor ML NK cells with lower Ki-67 expression failed treatment. However, in this small sample size, total donor

NK cell numbers in the PB at a single time point (7 days) measured post-infusion did not directly correlate with response (Fig. S1D). While these data provide insight into the mechanisms underlying treatment failure, they include a single time point and further studies are needed. These in vivo data are consistent with the in vitro observations that CD8α$^+$ ML NK cells do not proliferate as strongly as CD8α$^-$ ML NK cells, and may explain the inferior clinical responses.

To evaluate the cell-intrinsic role for CD8α on ML NK cell functionality, ΔCD8a ML NK cells were compared to WT ML NK cells in in vitro functional assays (Fig. 7J–M). Using this approach, CD8α expression was reduced on ΔCD8a ML NK cells compared to WT ML NK cells (Fig. 7K). K562 target killing by ΔCD8a ML NK cells was slightly, yet significantly, decreased compared to WT ML NK cells (Fig. 7L). Further, in response to cytokines and tumor targets, IFN-γ, TNF, and CD107a were similar between ΔCD8a ML NK cells, compared to WT ML NK cells (Fig. 7M). These data suggest that CD8α does not impair ML NK cell responses to prototypical stimuli, but further studies are warranted.

Discussion

Here we used multidimensional immune correlative phenotyping by mass cytometry to identify the in vivo differentiated human ML NK cell phenotype, which was distinct from cytokine-activated and conventional NK cells. ML NK cells were safe, expanded in vivo, and induced IWG responses in 67% (47% CR/CRi) of evaluable patients. We demonstrated that NKG2A is transcriptionally regulated in ML NK cells and represents a critical induced checkpoint for cytokine-induced ML NK cell responses, associating with treatment failure in AML patients treated with donor ML NK cells. Although little is known about the role of CD8α on NK cells, we identified a new association with CD8α$^+$ NK cellular therapy and inferior patient outcomes, likely due to their inability to robustly proliferate in response to combined cytokine activation.

NKG2A is a C-type lectin inhibitory receptor which heterodimerizes with CD94 and recognizes the non-classical class I-MHC HLA-E, resulting in ITIM-mediated NK cell inhibition (22). NKG2A expression on baseline donor NK cells was not associated with clinical outcomes. Furthermore, the importance of NKG2A for conventional (naïve) or control (low dose IL-15 supported) NK cell response to HLA-E$^+$ tumor targets was not observed, suggesting that NKG2A is a minor inhibitory receptor on conventional NK cells. Here we demonstrated that NKG2A is an inducible checkpoint molecule on cytokine-induced ML NK cells and is a critical inhibitor of ML NK cell responses against HLA-E positive tumor targets. NKG2A can be transcriptionally induced during memory-like differentiation. However both enhanced proliferation of NKG2A$^+$ NK cells and de novo NKG2A upregulation are likely operative in regulating overall NKG2A expression during ML NK cell differentiation. Our previous report showed that ML NK cells are not inhibited through the regular rules of inhibitory KIR to KIR-ligand interactions (5). Data presented here indicate that ML NK cells are instead primarily inhibited through NKG2A, and further studies examining the role for NKG2A and immune tolerance in the setting of cytokine-activation and inflammation are warranted. Moreover, the fraction of NKG2A$^+$ NK cells does not appear as important as the per cell NKG2A expression, since nearly all donor ML

NK cell expressed NKG2A, but only those donors with supra-physiologic expression were associated with treatment failure. However, HLA-E expression was overall increased in the treatment-failure tumor microenvironment, suggesting both NKG2A supra-expression and increased HLA-E contribute to resistance to ML NK cellular therapy. While future work will elucidate the mechanisms of supra-physiologic expression by some donors, we showed that NKG2A is transcriptionally induced after IL-12, IL-15, and IL-18 activation, and is associated with a concomitant increases in GATA-3, a known regulator of NKG2A, as well as Eomes, which is important for establishing a central memory phenotype in $CD8^+$ T cells (25). The interplay between these two transcription factors and how they establish ML NK cell differentiation program is unclear, but this is an active area for further investigation. Translationally, blockade of NKG2A or gene editing of *KLRC1* represent exciting potential strategies to improve on ML NK cellular therapy. Pre-clinical studies utilizing these approaches are ongoing and critical for establishing proof-of-principle needed to move this strategy into the clinic. Indeed, recent reports have demonstrated that combination anti-NKG2A and anti-PD-L1 mAb controlled tumor growth in a murine models of B and T-cell lymphoma, as well as established the safety of anti-NKG2A mAb for patients with squamous cell carcinoma of the head and neck (29), supporting the feasibility of translating our findings to the clinic.

There are limited reports of the role of CD8 on human NK cells, which is normally expressed as a CD8α homodimer, leaving CD8 receptor biology unclear in this context. Previous reports indicate that $CD8^+$ NK cells have enhanced cytotoxicity and undergo reduced activation induced-apoptosis (26,30). Additionally, the presence of $CD8^+$ NK cells have been associated with slower HIV-1 progression in chronically infected individuals (31). CD8α expression on NK cells was reported to contribute to KIR3DL1 signaling (32). Stronger CD8 interactions with MHC-I were hypothesized to improve licensing by enhancing KIR-KIR-ligand interactions, which is one possible mechanism for increasing NK cell functionality (32). However, our study implies a negative role for $CD8\alpha^+$ NK cells in adoptive NK cell immunotherapy. Potentially explaining this conundrum, we show that $CD8\alpha^+$ NK cells have reduced proliferative capacity compared to $CD8\alpha^-$ NK cells. Indeed, there are some studies examining the role of CD8αα in limiting T cell responses (33). CD8αβ is a well-characterized co-receptor for TCR interactions with MHC-I, and enhances TCR signaling (34). However, studies have implicated CD8αα as inhibiting T cell responses and that CD8αα may act as an inhibitory molecule in non-classical T cell subsets (33,35). While $CD8\alpha^+$ NK cells exhibit reduced proliferation, it remains unclear if CD8α is a marker of a differentiated, terminal phenotype with limited replicative capacity, or if CD8 is directly inhibiting proliferation in vivo. The negative association of CD8 expression with clinical outcomes following NK cell immunotherapy identifies the importance of understanding its role on NK cells, as well as the potentially distinct biology of $CD8\alpha^+$ NK cells from $CD8\alpha^-$ NK cells.

Here we report the first high dimensional characterization of in vivo differentiated ML NK cells in the context of the final phase 1 clinical data, demonstrating the safety and efficacy of ML NK cells to treat rel/ref AML patients. ML NK cells are well-tolerated and did not cause GVHD, cytokine release syndrome (CRS), or ICANS, nor ≥ grade 3 adverse events related to ML NK cell infusion. The observed CR/CRi rate of 47% is remarkable for a population of

older adults with rel/ref AML, and is consistent with our initial report. Although the duration of response was relatively short (2–6 months) for most patients, one patient, who became HCT eligible, had a durable response that persisted after allogeneic HCT. This strategy as a 'bridge to HCT' is being tested in our phase 2 cohort for rel/ref AML (NCT01898793). Based upon their ability to ignore inhibitory KIR ligation, we are also evaluating the effectiveness of ML NK cells against solid tumors (36), and expanding their repertoire against NK-resistant tumors using bi-specific triggering (37), as well as chimeric antigen receptor engineering (38). With our extensive immune correlative studies, we have identified NKG2A as a targetable checkpoint that could be combined with ML NK cell adoptive therapy in future trials. Moreover, a new strategy for donor NK cell donor selection based on $NKG2A^{+}CD8^{+}$ NK cell frequency was discovered. We have reported in preliminary form multiple clinical trials at Washington University utilizing ML NK cell adoptive immunotherapy, including as a bridge to HCT (NCT01898793), as augmentation of MHC-haploidentical HCT with same-donor ML NK cells (NCT02782546), and as therapy for relapse after allogeneic HCT (NCT03068819) (39,40). As evidenced by the current study, multidimensional immune correlates will be performed to understand if NKG2A and CD8 can predict patient outcomes in other ML NK cell clinical contexts. Thus, this study highlights the importance of multidimensional immune monitoring to identify mechanisms of response and resistance following NK cell therapy.

Materials and Methods

Study design

Patients treated on an open-label, non-randomized, phase 1 dose escalation trial (NCT01898793) are included in this study. Prior to any study-related testing or treatment, written informed consent was obtained from all patients under a Washington University School of Medicine Institutional Review Board-approved clinical protocol, and all studies were conducted in accordance with the Declaration of Helsinki. The initial escalation was previously reported (5). Briefly, patients were treated with fludarabine/cyclophosphamide between days −7 and −2 for immunosuppression, followed on day 0 by allogeneic donor IL-12, IL-15, and IL-18 activated NK cells. Patients in dose level 3 received the maximum NK cells that could be generated (capped at 10×10^6 cells/kg). After donor NK cell transfer, rhIL-2 was administered subcutaneously every other day for a total of 6 doses. Donor NK cells were purified from a non-mobilized apheresis product using CD3 depletion followed by CD56-positive selection (CliniMACS device). Purified NK cells were activated with IL-12 (10ng/mL), IL-15 (50 ng/mL), and IL-18 (50 ng/mL) for 12 hours under current GMP conditions.

Samples were obtained from the peripheral blood (day 7, 8 and 14 after infusion) and bone marrow (BM; screening, day 8 and 14 after infusion). Clinical responses were defined by the revised IWG criteria for AML (15). All patients provided written informed consent before participating and were treated on a Washington University Institutional Review Board (IRB)-approved clinical trial (Human Research Protection Office #201401085).

Reagents and cell lines

Anti-human monoclonal antibodies (mAb) were used for flow and mass cytometry (supplemental methods, Table S4). Endotoxin-free, recombinant human (rh) IL-12 (Biolegend), IL-15 (Miltenyi), and IL-18 (InVivo Gen) were used in these studies. K562 cells [American Type Culture Collection (ATCC), CCL-243] were obtained in 2008, viably cryopreserved, and maintained for <2 months at a time in continuous culture according to ATCC specifications. K562 were authenticated in 2015 using single-nucleotide polymorphism analysis and were found to be exactly matched to the K562 cells from the Japanese Collection of Research Bioresources, German Collection of Microorganisms, and Cell Cultures (DSMZ), and ATCC databases (Genetic Resources Core Facility at Johns Hopkins University). HLA-E^+ K562 were a gift from Dr. Bhattacharya. These cells were generated using the AAVS1-EF1a donor plasmid containing the coding sequence for human HLA-E. The K562 were electroporated using a Bio-Rad Gene Pulse electroporation system. HLA-E^+ cells were sorted to >98% purity.

NK cell purification and cell culture

Normal donor PBMCs were obtained from anonymous healthy platelet donors. NK cells were purified using RosetteSep (STEMCELL technologies; routinely >95% $CD56^+$ $CD3^-$). Memory-like and control NK cells were generated as previously described (5). Cells were maintained in 1 ng/mL IL-15, with media changes every 2–3 days. For proliferation assays, cells were labeled with 2.5 μM CellTrace violet (CTV, Life Technologies) for 15 minutes at 37C.

Patient Samples

Patients with newly diagnosed AML provided written informed consent under the Washington University IRB-approved protocol (Human Research Protection Office #2010–11766) and were the source of primary AML blasts for in vitro stimulation experiments. Patient PBMC and BMMC were isolated by Ficoll-Paque PLUS (GE Health) centrifugation and immediately used in experiments. For assessing HLA-E expression in patient BM, viably frozen cells were thawed and stained immediately using mass cytometry.

Functional assays to assess cytokine production

For patient stimulation assays, PBMC or BM cells were stimulated in a standard functional assay (5). Cells were stimulated with K562 leukemia targets (5:1 effector to target ratio). Functionality was measured using mass cytometry as previously described (5). For each patient sample, a normal donor sample was thawed and stimulated with K562 and used as a control for the functional assay. For in vitro differentiated NK cell functional assays, control and memory-like NK cells were harvested after a rest period of 5–7 days to allow memory-like NK cell differentiation to occur. Cells were incubated with K562 ± HLA-E or freshly thawed primary AML blasts. All cytokine secretion assays were performed for 6 hours in the presence of GolgiPlug/GolgiStop (BD) for the final 5 hours. Anti-CD107a antibodies were included in the well at the beginning of the assay to measure degranulation. For antibody blocking experiments, 10 μg/mL anti-NKG2A (Z199), anti-NKG2C (134522) or isotype control (IgG) were added directly to the wells at the beginning of the assay.

Flow-based killing assay

Flow-based killing assays were performed by co-incubating memory-like or control NK cells with carboxyfluorescein succinimidyl ester (CFSE)-labeled K562 ± HLA-E for 4 hours and assaying 7-aminoactinomycin D (7AAD) uptake as described (13).

qRT-PCR

Cells were resuspended in Trizol and RNA extracted using Zymo Directzol RNA microPrep according to manufacturer's directions. cDNA was generated using Life Technologies high capacity cDNA reverse transcription kit (4368814) according to manufacturer's instructions. Real-time qPCR was performed using ABI master mix with TaqMan Gene Expression Assay, Hs00970273_g1 KLRC1, Hs00935338_m1 BACH2, and Hs01060665_g1 ACTB, according to manufacturer's instructions. Samples were analyzed on StepOnePlus Real-Time PCR system (Applied Biosystems). Relative quantification was determined by ΔΔ threshold cycle method, by normalizing KLRC1 or BACH2 to ACTB (beta-actin).

RNA-sequencing and GSEA

Cells were stored in Trizol at −80°C until RNA isolation using the Direct-zol RNA MicroPrep kit (Zymo Research). NextGen RNA sequencing was performed using an Illumina HiSeq 2500 sequencer. RNA-seq reads were then aligned to the Ensembl release 76 primary assembly with STAR version 2.5.1a. Gene counts were derived from the number of uniquely aligned unambiguous reads by Subread:featureCount version 1.4.6-p5. Analysis of sequencing data was performed using Phantasus, a browser-based gene expression analysis software. Genes were log2 normalized and filtered to remove duplicate reads and lowly-expressed genes. Differential expression analysis was performed on the top 12,000 expressed genes using the LIMMA package to analyze differences between conditions. Gene-set enrichment analysis was performed using the Harmonizome database of GATA3 target genes (41).

Flow cytometric analysis and sorting

Cell staining was performed as described (5) and data were acquired on a Gallios flow cytometer (Beckman Coulter) and analyzed using FlowJo (Tree Star) software. Dead cells were stained using Zombie reagent (Biolegend) according to manufacturer's instructions, except for phosphor-flow. eBio Fix/Perm was used for all intracellular staining except phospho-flow. For phospho-flow, cells were stimulated with IL-12, IL-15, and IL-18 for 0, 15, 60, and 120 minutes. Cells were fixed in 1% pre-warmed formalin and permeabilized using 100% ice cold methanol. Cells were washed 3 times and stained overnight, as previously described (42). $CD8^+$ and $CD8^-$ NK cells were sorted to >99% purity using FACSAria II cell sorter (BD Biosciences) or purified using Automacs column (Miltenyi). $CD56^{Dim}$ $CD16^+$ $NKG2A^+$ and $NKG2A^-$ NK cells were sorted using FACSAria II cell sorter (BD Biosciences).

Mass cytometry

Mass cytometry was performed on freshly isolated patient PB or BM cells as previously described (5,43), or on thawed BM samples. Cells were stained for live/dead using cisplatin,

and surface staining performed at 4C for 15 minutes. Cells were washed, fixed with eBio Fix/Perm overnight at 4C. Cells were stained using intracellular antibodies at 4C for 15 minutes. Cells were washed and resuspended in PBS containing 1% PFA and stored until all samples were stained. Once all samples were stained, they were washed and barcoded according to manufacturer's instructions. Data were collected on a Helios mass cytometer (Fluidigm) and analyzed using Cytobank (44). Data were analyzed using previously described methods (45). KIR diversity (KIR2DL1, KIR2DL2/2DL3, KIR3DL1, KIR2DS4, KIR2DL5) was assessed at baseline and after in vivo differentiation as previously described (5). For each patient sample, a normal donor PBMC sample was thawed and stained, providing a staining control at Day 0, Day 7 and Day 8 of patient sample staining. These were used for quality control. Staining for each marker was confirmed to be consistent across the days on which the samples were stained using the same master mix. Comparisons were also made (Student's t test or Mann-Whitney) between matched normal donors stained on D0 and D7. For all markers, there were not significant differences in median expression between normal donors thawed and stained on D0 or D7. These control samples serve to increase our confidence that changes we observe in our patient samples represent biologically relevant changes and do not reflect technical issues that could arise from these assays. Citrus was performed assessing median with default settings, using the same clustering channels as the viSNE (Fig. 1, Table S4), with the addition of CD8. To define the in vivo memory-like differentiated phenotype (Fig 1.) and the lymphocyte subsets, we used all patient with mass cytometry data available, including CIML026 who expired prior to day 28, post-infusion, and was thus not evaluable for response (male, aged 77, diagnosed with AML, treated at dose level 3, 2 prior therapies, 7% blasts prior to treatment). CIML025 was evaluable but was treated at a dose level 2 and was excluded from the Citrus analyses (Fig. 5, Fig. 7). Phenotypic intracellular markers for CIML028 were not assessed. For CIML020, an inappropriate amount of Ki-67 antibody was used, making the median expression value an outlier (ROUT [Q=1%]), however, percent positive could still be reliably assessed. For functional assays, CD107a was omitted from the functional assay for CIML026. For patient CIML027, due to limiting cells in the PB, bone marrow donor NK cells were used to assess licensing. CIML028 had only had cells available for a functional assay at D14.

CRISPR/Cas9 gene editing

NK cells were purified from normal donors and rested overnight in 1 ng/mL IL-15. Cells were washed with PBS, 2 times to remove serum, and resuspended in MaxCyte EP buffer plus CAS9 mRNA (Trilink) (46). Next, gRNA [NKG2A: AACAACUAUCGUUAACCACAG (Trilink, Synthego); EOMES: AACCAGUAUUAGGAGACUCU (IDT); or CD8A: GACUUCCGCCGAGAGAACGA (IDT)] (2×10^8 cells/ml) or no gRNA (control) was added to the cells which were then electroporated in a Maxcyte GT using the WUSTL-2 setting in an OC-100 processing assembly. Cells were removed from the OC-100 and incubated for 10 minutes at 37°C. Pre-warmed media containing 3 ng/mL IL-15 was added and cells rested for 24 hours. Cells were then control treated (3 ng/mL IL-15) or cytokine activated (IL-12/15/18) for 16–18 hours, as previously described (10). Cells were washed 3 times and maintained in complete RPMI supplemented with 10% Human AB serum and 3 ng/mL IL-15. Media changes were

performed every 2–3 days. Gene editing efficiency was determined as previously described (Fig. S11A–B) (47).

Statistical analysis

Before statistical analyses, all data were tested for normal distribution (Shapiro-Wilk). If data were not normally distributed, the appropriate non-parametric tests were used (GraphPad Prism v8), with all statistical comparisons indicated in the figure legends. Uncertainty is represented in figures as SEM, except where indicated. All comparisons used a two-sided α of 0.05 for significance testing.

Supplementary Material

Refer to Web version on PubMed Central for supplementary material.

Acknowledgments:

We would like to thank our patient volunteers and the HCT/leukemia physician and nursing teams who care for them at the Washington University School of Medicine (WUSM). We acknowledge support from the Genome Engineering and iPSC Center (GEiC) at WUSM for gRNA validation services, as well as the Siteman Flow Cytometry Core (Bill Eades), Immune Monitoring Lab (Stephen Oh), and Biological Therapy Core Facility of the Siteman Cancer Center. We thank the Genome Technology Access Center in the Department of Genetics at Washington University School of Medicine for help with genomic analysis. The Center is partially supported by NCI Cancer Center Support Grant #P30 CA91842 to the Siteman Cancer Center and by ICTS/CTSA Grant# UL1TR002345 from the National Center for Research Resources (NCRR), a component of the National Institutes of Health (NIH), and NIH Roadmap for Medical Research. This publication is solely the responsibility of the authors and does not necessarily represent the official view of NCRR or NIH. Figure 1a illustration by Astrid Rodriguez Velez and Anne Robinson in association with InPrint at Washington University in St. Louis.

Funding: National Institutes of Health (NIH/NHLBI): T32HL00708843 (J. Wagner, P. Wong); (NIH/NCI): F32CA200253 (M. Berrien-Elliott), K12CA167540 (M. Berrien-Elliott), P50CA171063 (M. Berrien-Elliott, A. Cashen, T. Fehniger), R01CA205239 (T. Fehniger). Additional funding from the Leukemia and Lymphoma Society (T. Fehniger), V Foundation for Cancer Research (T. Fehniger), The American Association of Immunologists Intersect Fellowship Program for Computational Scientists and Immunologists (J. Foltz, T. Fehniger), and the Children's Discovery Institute (CDI) at WUSM (T. Fehniger).

References and Notes:

1. Vivier E, Tomasello E, Baratin M, Walzer T, Ugolini S. Functions of natural killer cells. Nat Immunol. Nature Publishing Group; 2008;9:503–10.
2. Lanier LL. NK cell recognition. Ann Rev Immunol. Annual Reviews; 2005;23:225–74.
3. Estey E, Döhner H. Acute myeloid leukaemia. Lancet. 2006;368:1894–907. [PubMed: 17126723]
4. Miller JS, Soignier Y, Panoskaltsis-Mortari A, McNearney SA, Yun GH, Fautsch SK, et al. Successful adoptive transfer and in vivo expansion of human haploidentical NK cells in patients with cancer. Blood. American Society of Hematology; 2005;105:3051–7.
5. Romee R, Rosario M, Berrien-Elliott MM, Wagner JA, Jewell BA, Schappe T, et al. Cytokine-induced memory-like natural killer cells exhibit enhanced responses against myeloid leukemia. Sci Transl Med. American Association for the Advancement of Science; 2016;8:357ra123–357ra123.
6. Shimasaki N, Jain A, Campana D. NK cells for cancer immunotherapy. Nat Rev Drug Discov. 2020;19:200–18. [PubMed: 31907401]
7. Berrien-Elliott MM, Romee R, Fehniger TA. Improving natural killer cell cancer immunotherapy. Curr Opin Organ Transplant. 2015;20:671–80. [PubMed: 26414502]
8. Hirayama AV, Turtle CJ. Toxicities of CD19 CAR-T cell immunotherapy. Am J Hematol. 2019;94:S42–9. [PubMed: 30784102]

9. Simonetta F, Pradier A, Bosshard C, Masouridi-Levrat S, Chalandon Y, Roosnek E. NK Cell Functional Impairment after Allogeneic Hematopoietic Stem Cell Transplantation Is Associated with Reduced Levels of T-bet and Eomesodermin. J Immunol. The American Association of Immunologists; 2015;195:4712–20.
10. Romee R, Schneider SE, Leong JW, Chase JM, Keppel CR, Sullivan RP, et al. Cytokine activation induces human memory-like NK cells. Blood. The American Society of Hematology; 2012;120:4751–60.
11. Ni J, Miller M, Stojanovic A, Garbi N, Cerwenka A. Sustained effector function of IL-12/15/18-preactivated NK cells against established tumors. J Exp Med. 2012;209:2351–65. [PubMed: 23209317]
12. Cooper MA, Elliott JM, Keyel PA, Yang L, Carrero JA, Yokoyama WM. Cytokine-induced memory-like natural killer cells. Proc Natl Acad Sci U S A. National Academy of Sciences; 2009;106:1915–9.
13. Leong JW, Chase JM, Romee R, Schneider SE, Sullivan RP, Cooper MA, et al. Preactivation with IL-12, IL-15, and IL-18 induces CD25 and a functional high-affinity IL-2 receptor on human cytokine-induced memory-like natural killer cells. Biol Blood Marrow Transpl. Elsevier Ltd; 2014;20:463–73.
14. Wagner JA, Berrien-Elliott MM, Rosario M, Leong JW, Jewell BA, Schappe T, et al. Cytokine-Induced Memory-Like Differentiation Enhances Unlicensed NK Cell Anti-Leukemia and FcγRIIIa-Triggered Responses. Biol Blood Marrow Transplant. Elsevier Inc; 2016;23:398–404.
15. Cheson BD, Bennett JM, Kopecky KJ, Buchner T, Willman CL, Estey EH, et al. Revised recommendations of the International Working Group for Diagnosis, Standardization of Response Criteria, Treatment Outcomes, and Reporting Standards for Therapeutic Trials in Acute Myeloid Leukemia. J Clin Oncol. 2003;21:4642–9. [PubMed: 14673054]
16. Van Gassen S, Callebaut B, Van Helden MJ, Lambrecht BN, Demeester P, Dhaene T, et al. FlowSOM: Using self-organizing maps for visualization and interpretation of cytometry data. Cytom Part A. 2015;87:636–45.
17. Bachanova V, Burns LJ, McKenna DH, Curtsinger J, Panoskaltsis-Mortari A, Lindgren BR, et al. Allogeneic natural killer cells for refractory lymphoma. Cancer Immunol Immunother. 2010;59:1739–44. [PubMed: 20680271]
18. Gumá M, Angulo A, Vilches C, Gómez-Lozano N, Malats N, Lopez-Botet M, et al. Imprint of human cytomegalovirus infection on the NK cell receptor repertoire. Blood. 2004;104:3664–71. [PubMed: 15304389]
19. Foley B, Cooley S, Verneris MR, Pitt M, Curtsinger J, Luo X, et al. Cytomegalovirus reactivation after allogeneic transplantation promotes a lasting increase in educated NKG2C+ natural killer cells with potent function. Blood. 2011;612–26. [PubMed: 22042695]
20. Horowitz A, Strauss-Albee DM, Leipold M, Kubo J, Nemat-Gorgani N, Dogan OC, et al. Genetic and environmental determinants of human NK cell diversity revealed by mass cytometry. Sci Transl Med. 2013;5:208ra145.
21. Bruggner RV, Bodenmiller B, Dill DL, Tibshirani RJ, Nolan GP. Automated identification of stratifying signatures in cellular subpopulations. Proc Natl Acad Sci USA. 2014;111:E2770–7. [PubMed: 24979804]
22. Lee N, Llano M, Carretero M, Ishitani A, Navarro F, López-Botet M, et al. HLA-E is a major ligand for the natural killer inhibitory receptor CD94/NKG2A. Proc Natl Acad Sci USA. 1998;95:5199–204. [PubMed: 9560253]
23. Björkström NK, Riese P, Heuts F, Andersson S, Fauriat C, Ivarsson M a, et al. Expression patterns of NKG2A, KIR, and CD57 define a process of CD56dim NK-cell differentiation uncoupled from NK-cell education. Blood. 2010;116:3853–64. [PubMed: 20696944]
24. Marusina AI, Kim D-K, Lieto LD, Borrego F, Coligan JE. GATA-3 Is an Important Transcription Factor for Regulating Human NKG2A Gene Expression. J Immunol. 2005;174:2152–9. [PubMed: 15699146]
25. Banerjee A, Gordon SM, Intlekofer AM, Paley MA, Mooney EC, Lindsten T, et al. Cutting edge: The transcription factor eomesodermin enables CD8+ T cells to compete for the memory cell niche. J Immunol. 2010;185:4988–92. [PubMed: 20935204]

26. Addison EG, North J, Bakhsh I, Marden C, Haq S, Al-Sarraj S, et al. Ligation of CD8alpha on human natural killer cells prevents activation-induced apoptosis and enhances cytolytic activity. Immunology. 2005;116:354–61. [PubMed: 16236125]
27. Leonard WJ, Lin J-X. Cytokine receptor signaling pathways. J Allergy Clin Immunol. 2000;105:877–88. [PubMed: 10808165]
28. Li Q, Verma IM. NF-κB regulation in the immune system. Nat Rev Immunol. 2002;2:725–34. [PubMed: 12360211]
29. André P, Denis C, Soulas C, Bourbon-Caillet C, Lopez J, Arnoux T, et al. Anti-NKG2A mAb Is a Checkpoint Inhibitor that Promotes Anti-tumor Immunity by Unleashing Both T and NK Cells. Cell. 2018;175:1731–1743.e13. [PubMed: 30503213]
30. Srour EF, Leemhuis T, Jenski L, Redmond R, Jansen J. Cytolytic activity of human natural killer cell subpopulations isolated by four-color immunofluorescence flow cytometric cell sorting. Cytometry. 1990;11:442–6. [PubMed: 2187659]
31. Ahmad F, Hong HS, Jackel M, Jablonka A, Lu I-N, Bhatnagar N, et al. High Frequencies of Polyfunctional CD8+ NK Cells in Chronic HIV-1 Infection Are Associated with Slower Disease Progression. J Virol. 2014;88:12397–408. [PubMed: 25122796]
32. Geng J, Raghavan M. CD8αα homodimers function as a coreceptor for KIR3DL1. Proc Natl Acad Sci. 2019;116:17951–6. [PubMed: 31420518]
33. Cheroutre H, Lambolez F. Doubting the TCR Coreceptor Function of CD8αα. Immunity. 2008;28:149–59. [PubMed: 18275828]
34. Artyomov MN, Lis M, Devadas S, Davis MM, Chakraborty AK. CD4 and CD8 binding to MHC molecules primarily acts to enhance Lck delivery. Proc Natl Acad Sci. 2010;107:16916–21. [PubMed: 20837541]
35. Cawthon AG, Lu H, Alexander-Miller MA. Peptide Requirement for CTL Activation Reflects the Sensitivity to CD3 Engagement: Correlation with CD8αβ Versus CD8αα Expression. J Immunol. 2001;167:2577–84. [PubMed: 11509598]
36. Marin-Agudelo NM, Krasnick B, Becker-Hapak M, Berrien-Elliott MM, Foster M, Marsala LM, et al. Cytokine-induced memory-like NK cells exhibit enhanced autologous responses to metastatic melanoma. Soc Nat Immun. 2019.
37. Marin N, Becker-Hapak M, Koch J, Berrien-Elliott MM, Foster M, Neal C, et al. Abstract 1546: The CD30/CD16A bispecific innate immune cell engager AFM13 elicits heterogeneous single-cell NK cell responses and effectively triggers memory-like (ML) NK cells Immunology. American Association for Cancer Research; 2019 page 1546–1546.
38. Gang M, Marin ND, Wong P, Neal CC, Marsala L, Foster M, et al. CAR-modified memory-like NK cells exhibit potent responses to NK-resistant lymphomas. Blood. 2020;In PressDOI: 10.1182/blood.2020006619.
39. Foltz JA, Berrien-Elliott MM, Neal C, Foster M, McClain E, Schappe T, et al. Cytokine-Induced Memory-like (ML) NK Cells Persist for > 2 Months Following Adoptive Transfer into Leukemia Patients with a MHC-Compatible Hematopoietic Cell Transplant (HCT) Blood. ASH; 2019;134:1954–1954.
40. Bednarski J, Zimmerman C, Cashen AF, Desai S, Foster M, Schappe T, McClain E, Becker-Hapak M, Berrien-Elliott MM, Fehniger TA, MD P. Adoptively Transferred Donor-Derived Cytokine Induced Memory-like NK Cells Persist and Induce Remission in Pediatric Patient with Relapsed Acute Myeloid Leukemia after Hematopoietic Cell Transplantation. Blood. 2019;134:A3307.
41. Rouillard AD, Gundersen GW, Fernandez NF, Wang Z, Monteiro CD, McDermott MG, et al. The harmonizome: a collection of processed datasets gathered to serve and mine knowledge about genes and proteins. Database. 2016, 2016, baw100, 10.1093/database/baw100. [PubMed: 27374120]
42. Wagner JA, A., Rosario M, Romee R, Berrien-Elliott MM, M., et al. CD56bright NK cells exhibit potent antitumor responses following IL-15 priming. J Clin Invest. 2017;127:4042–58. [PubMed: 28972539]
43. Romee R, Cooley S, Berrien-Elliott MM, Westervelt P, Verneris MR, Wagner JE, et al. First-in-human phase 1 clinical study of the IL-15 superagonist complex ALT-803 to treat relapse after transplantation. Blood. 2018;131:2515–27. [PubMed: 29463563]

44. Kotecha N, Krutzik PO, Irish JM. Web-based analysis and publication of flow cytometry experiments. Curr Protoc Cytom. 2010;Chapter 10:Unit10.17.

45. Diggins KE, Ferrell PB, Irish JM. Methods for discovery and characterization of cell subsets in high dimensional mass cytometry data. Methods. 2015;82:55–63. [PubMed: 25979346]

46. Cooper ML, Choi J, Staser K, Ritchey JK, Devenport JM, Eckardt K, et al. An “off-the-shelf” fratricide-resistant CAR-T for the treatment of T cell hematologic malignancies. Leukemia. 2018;32:1970–83. [PubMed: 29483708]

47. Clement K, Rees H, Canver MC, Gehrke JM, Farouni R, Hsu JY, et al. CRISPResso2 provides accurate and rapid genome editing sequence analysis. Nat Biotechnol. 2019;37:224–6. [PubMed: 30809026]

Statement of Significance

Mass cytometry reveals an in vivo memory-like NK cell phenotype, where NKG2A is a dominant checkpoint, and CD8α is associated with treatment failure after memory-like NK cell therapy. These findings identify multiple avenues for optimizing memory-like NK cell immunotherapy for cancer and define mechanisms important for memory-like NK cell function.

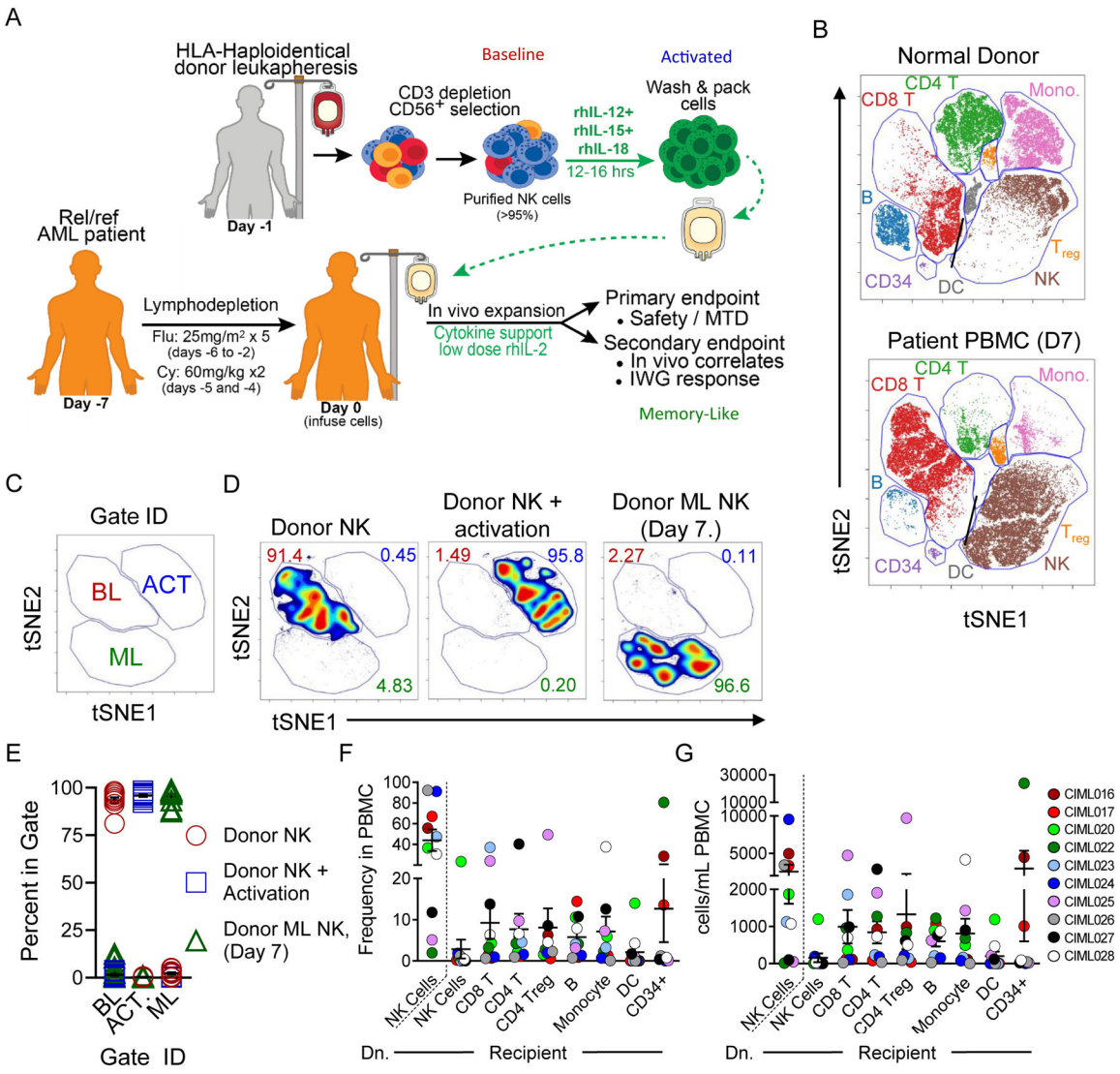

Fig. 1. In vivo differentiated cytokine-induced memory-like (ML) NK cells are distinct from conventional and cytokine-activated NK cells.

(**A**) Clinical trial schema. (**B-G**) Mass cytometry analysis of patient PBMC 7 days post-NK cell infusion reveal unique multidimensional phenotype and predominance of donor ML NK cells. Baseline (blue), activated (red), and memory-like (green) NK cell samples are indicated. (**B**) Representative viSNE plot of PBMC from a normal donor and a patient, 7 days after NK cell infusions (D7). FlowSOM identified populations are indicated. (**C-E**) viSNE analyses were performed on $CD45^{+}CD34^{-}CD14^{-}CD19^{-}CD3^{-}CD56^{+}HLA^{donor}$ NK cells after enrichment ($CD56^{+}$ Donor), activation, and 7 days after NK cell infusion (Donor ML NK). (**C**) Distinct populations were identified on viSNE maps based on clustering with 25 markers; baseline (BL), activated (ACT), and memory-like (ML). (**D**) Representative viSNE plots of one donor. Numbers indicate the frequency of NK cells that fall within the gate. (**E**) Summary data from (**D**) of BL, ACT, and ML NK cells, demonstrating consistent NK cell changes across donors. (**F**) Summary data from all patients showing frequency of FlowSOM gated populations from (B); Dn., donor NK cells, as determined by HLA-marker

expression. (**G**) Summary total cell populations from all patients. For summary data, lines represent the mean and error is represented as SEM.

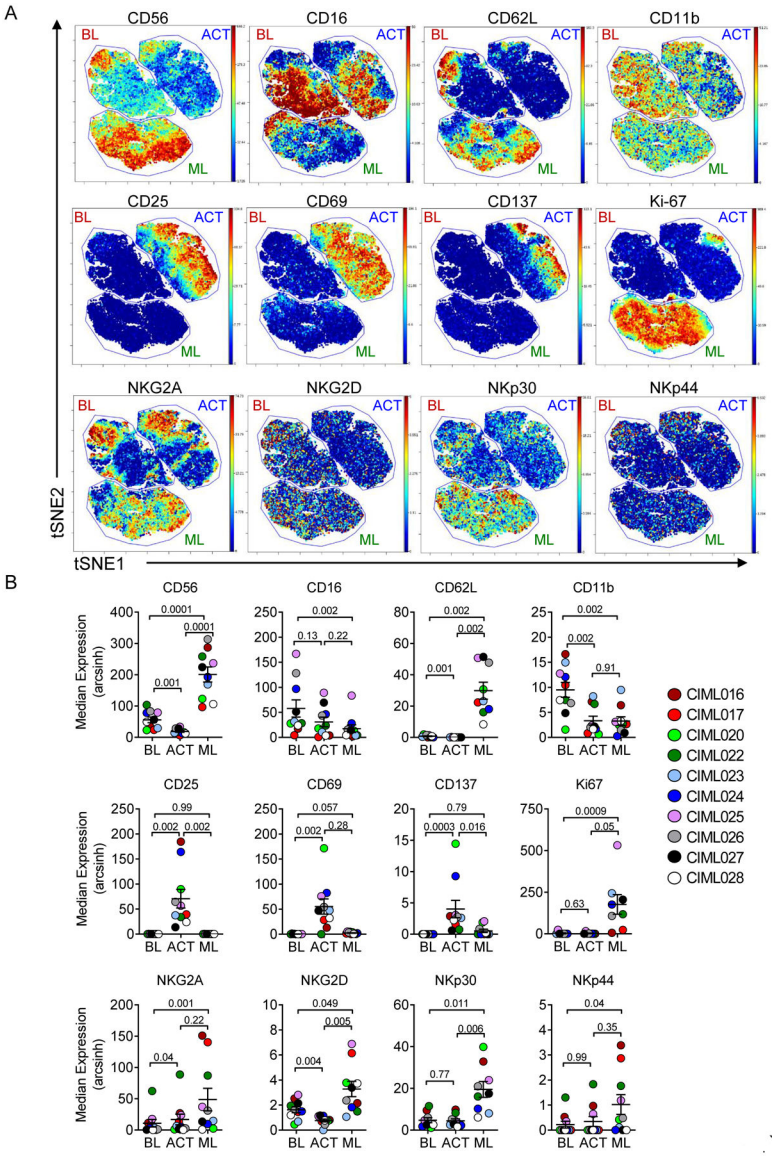

Fig. 2. Mass cytometry reveals distinct phenotypic changes after activation and in vivo memory-like NK cell differentiation.

(**A**) Representative viSNE maps showing BL, ACT, and ML NK populations, as defined in Fig. 1. Plot colors represent the median expression of the indicated marker. (**B**) Summary from (A). Data were tested for normal distribution using Shapiro-Wilk test. Normally distributed data were analyzed using RM-ANOVA with Holm-Sidak correction for multiple comparisons. Non-parametric data were analyzed using Friedman test with Dunn's multiple test correction. Lines represent the mean and error is represented as SEM.

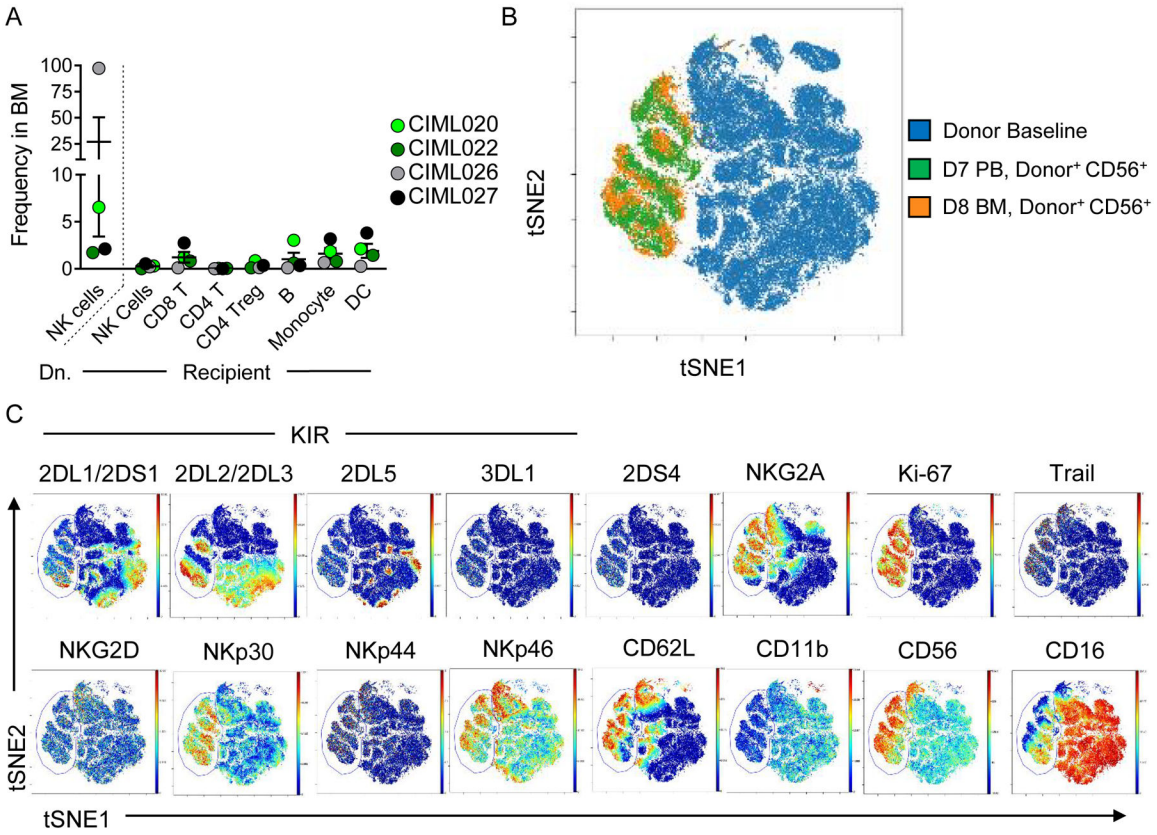

Fig. 3. Donor in vivo differentiated ML NK cells traffic to the BM and are phenotypically similar to PB ML NK cells.

(**A**) Summary data from Citrus-gated lymphocyte populations in patients with bone marrow (BM) assessed by mass cytometry at day 8 post NK cell infusion. (**B**) viSNE overlay of donor NK cells at BL (blue), donor NK cells in the PB (green), and donor ML NK cells in the BM, using the same clustering as in (Fig. 1–2). (**C**) Representative expression of indicated markers in BL NK cells and donor ML NK cells (indicated within the gate) from the PB and BM.

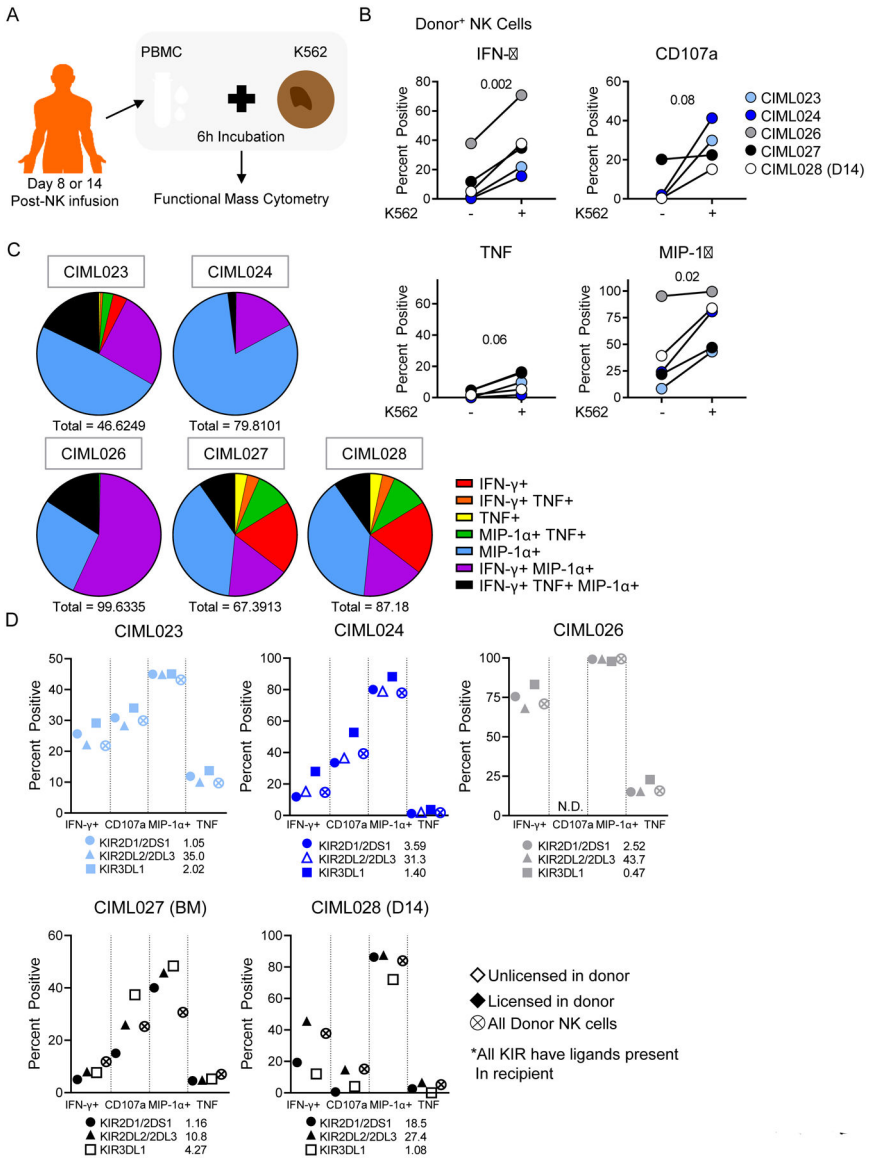

Fig. 4. Donor ML NK exhibit polyfunctional responses to leukemia targets ex vivo.

(**A**) Functional assay schema. Briefly, patient PBMC were collected 8 (n=4) or 14 (n=1) days after NK cell infusion. Lymphocytes were isolated, stimulated with K562, and assessed for the indicated markers by mass cytometry. (**B**) Frequency of donor NK cells producing the indicated protein after K562 stimulation. Data were analyzed using paired t test (parametric) or Wilcoxon (non-parametric). P-values are indicated within the graph. (**C**) Poly-functional responses from patient's donor NK cells. Total indicates the frequency of cells producing at least one cytokine/chemokine. (**D**) Functionality by licensing status is indicated for donor NK Cells. Solid symbols indicate the KIR was licensed in the donor, open symbols indicate the KIR was unlicensed in the donor. All KIR are predicated to be licensed in the patient. The frequency of each single KIR^+ subset is indicated for each KIR within each donor (below the graph). These data indicate that unlicensed ML NK cells are functional.

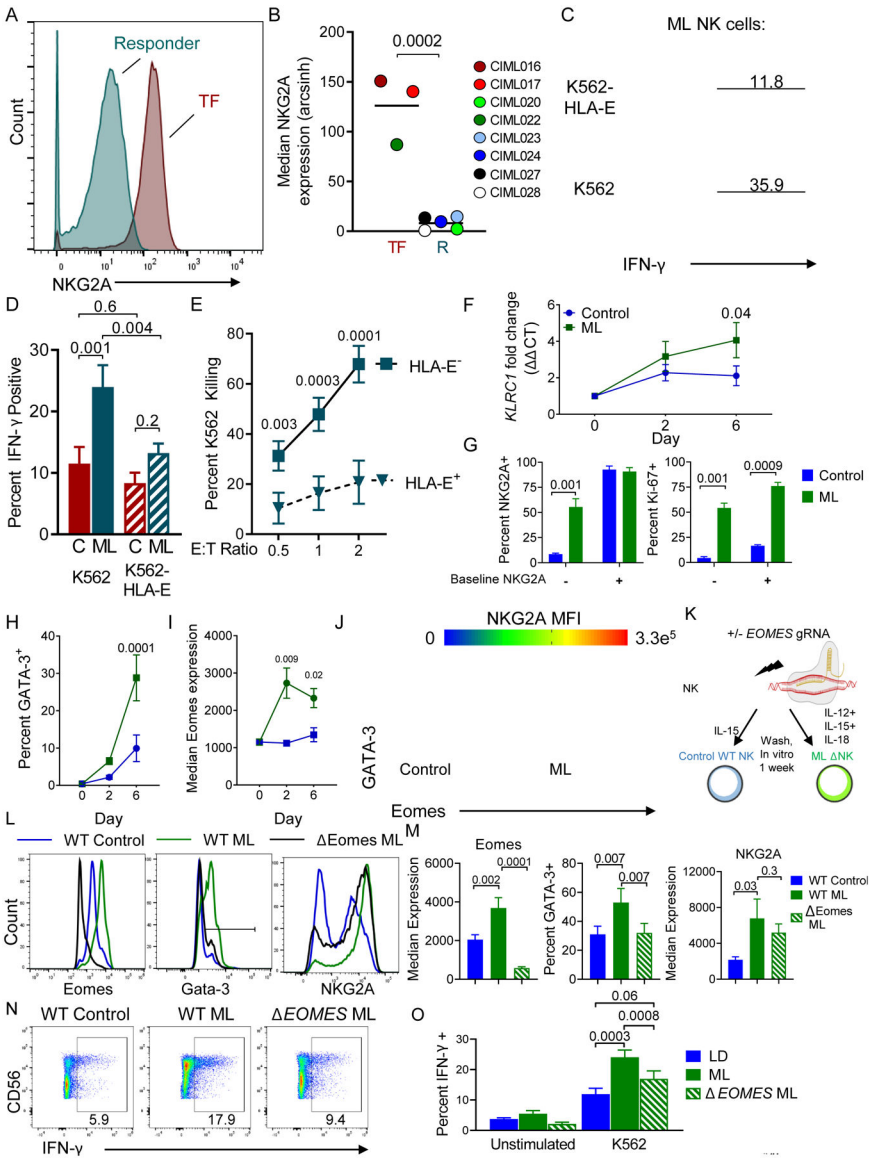

Fig. 5. Markedly increased NKG2A expression on ML NK cells within patient PBMC at day 7 is associated with treatment failure.

(**A**) Representative histogram of NKG2A expression on donor NK cells from a responder (R) or treatment-failure (TF) patient. (**B**) Summary data of median NKG2A expression on R v TF patients (n = 5 and 3, respectively). Data are shown with box-whiskers graph, with bars indicating min to max. Data were compared using Mann-Whitney test. (**C-J**) Control and memory-like NK cells were generated from normal donors in vitro and assessed. (**C**) Representative histograms showing IFN-γ expression by ML NK cells triggered with the indicated targets for 6 hours. Inset numbers depict percent IFN-γ^+. (**D**) Summary showing the frequency of IFN-γ^+ cells from ML and control (C) NK cells triggered with the indicated targets. Mean and SEM are shown, data were compared with RM-ANOVA with Holm-Sidak correction for multiple comparisons. (**E**) ML NK cell killing of K562 or HLA-E^+ K562 tumor targets at the indicated effector to target (E:T) ratio. (**F**) qRT-PCR showing *KLRC1* increases in ML NK cells compared to control cells. (**G**) Normal donor $CD56^{dim}$

$CD16^+$ cells were flow sorted based on NKG2A expression. Control or ML NK cells were assessed at day 7 for NKG2A expression (left) and Ki-67 (right). Summary data from 4–5 normal donors from 2–3 independent experiments. Mean and SEM are depicted and data were compared using 2way ANOVA. (**H**) Flow cytometry data showing the percent GATA-3^+ NK cells over time in control or ML NK cells. (**I**) Median Eomes expression data from control and ML NK cells. H-I data are mean and SEM, compared using 2way ANOVA with Sidaks correction. (**J**) Representative plot showing co-expression of GATA-3, Eomes, and colored by NKG2A Median fluorescence intensity (MFI). Gates enclose the GATA-3^+Eomes$^+$ NK cells. (**K**-**O**) Using CRISPR/Cas9, Eomes was deleted from NK cells prior to ML NK cell differentiation. Control, WT ML, and ΔEomes ML NK cells were generated in vitro and assessed after 7 days. (**K**) CRISPR/Cas9 Schema. (**L**) Representative histograms showing expression of indicated markers. (**M**) Summary from (L). (**N**-**O**) Representative flow plots showing IFN-γ production in response to K562 targets. Numbers represent the frequency of cells within the indicated gate. (**O**) Summary from (N). (L-O) Mean and SEM are displayed, data were compared using RM-ANOVA. N= 6 normal donors from 4 independent experiments, p-values are indicated within the graphs.

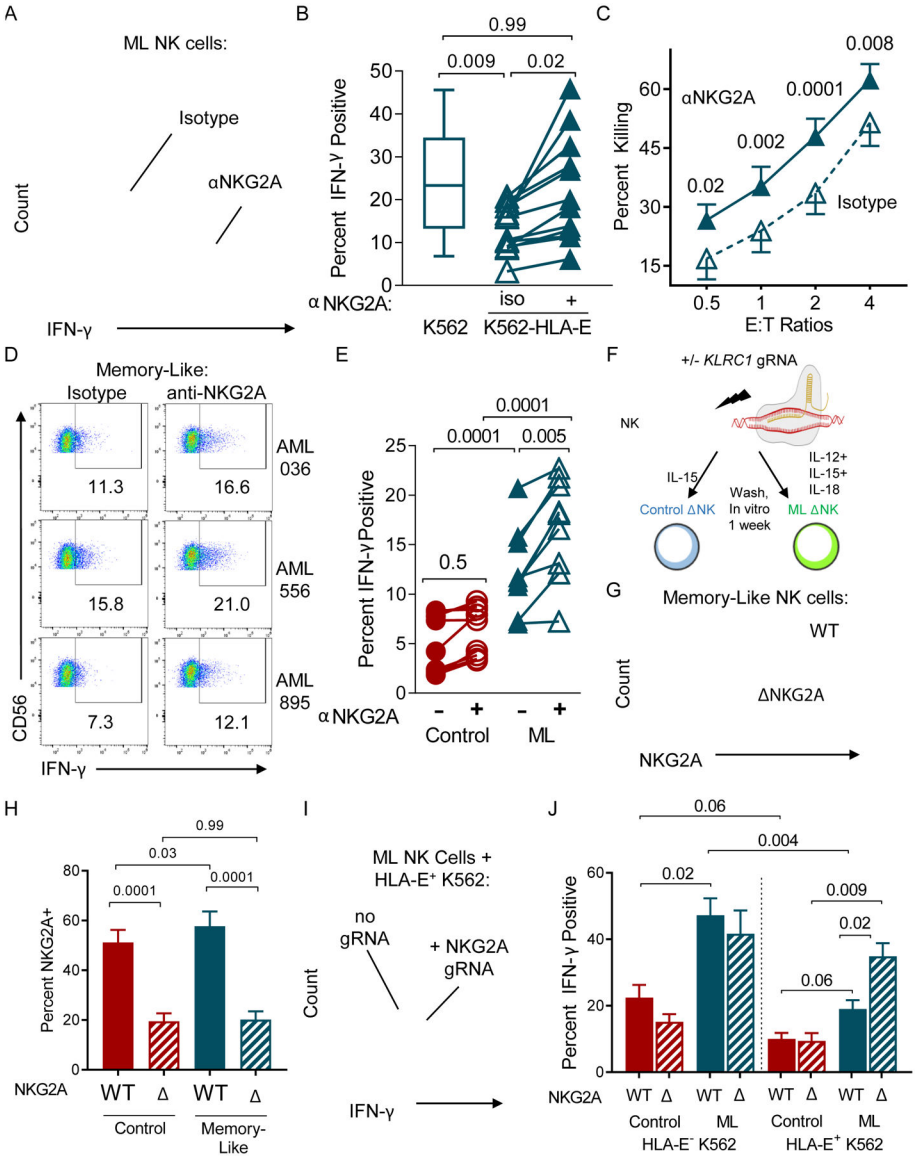

Fig. 6. Preventing NKG2A: HLA-E interactions restore ML NK cell responses to HLA-E$^+$ tumor targets.

Memory-like or control NK cells were generated in vitro and stimulated with K562 or K562-HLA-E$^+$. (**A**) Representative histogram showing IFN-γ expression in ML NK cells stimulated with K562-HLA-E$^+$ targets in the presence of isotype of anti-NKG2A antibody. (**B**) Summary data of ML NK cells stimulated with K562 or K562-HLA-E$^+$ with isotype or anti-NKG2A antibody. (**C**) K562-HLA-E$^+$ target killing by ML NK cells incubated with isotype or anti-NKG2A antibody. Mean and SEM are displayed. (**D**) Representative flow cytometry data assessing intracellular IFN-γ production by NK cells stimulated with primary AML in the presence of isotype or anti-NKG2A antibody. (**E**) Summary data from (D). Data were compared using a 2way ANOVA. (**F-J**) NKG2A protein expression was reduced using CRISPR/Cas9 and gRNA to KLRC1, then ML or control NK cells were generated in vitro and stimulated. (**F**) Experimental Schema. (**G**) Representative histogram of ML NK cells electroporated with NKG2A gRNA (bottom) compared to control treated

ML NK Cells. (**H**) Summary data showing percent NKG2A$^+$ NK cells. (**I-J**) Control or ΔNKG2A ML NK cells were incubated with K562-HLA-E$^+$ and IFN-γ measured. (**I**) Representative histogram showing NKG2A$^+$ ML NK cell and ΔNKG2A ML NK cell IFN-γ production. (**J**) Summary data from (I). Data are represented as mean and SEM. Data were compared using RM one-way ANOVA, and p-values are indicated within the graphs.

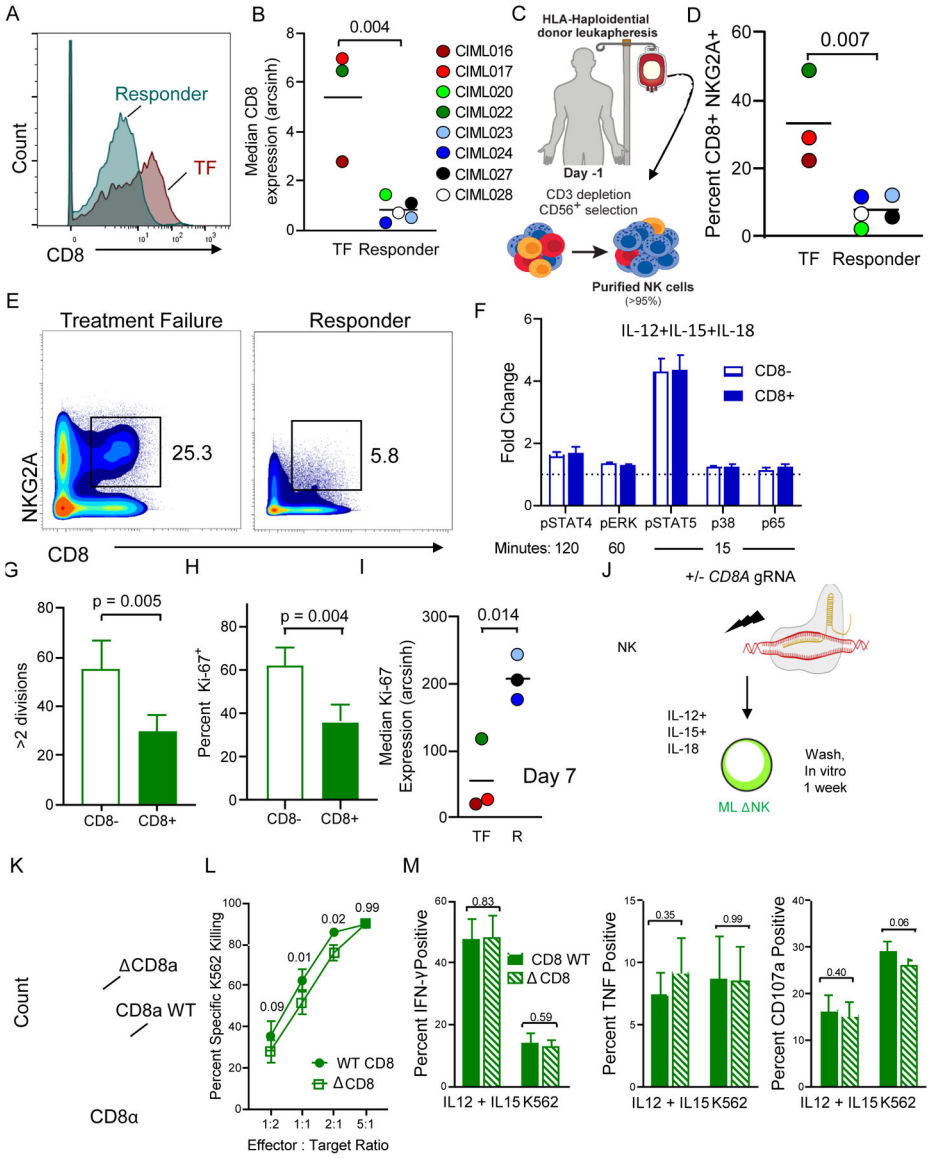

Fig. 7. CD8 expression on ML NK cells from patient PBMC at day 7 is associated with treatment failure.

(**A**) Representative histogram of CD8 expression on donor NK cells from responder (R) and a treatment-failure (TF) patient. (**B**) Summary data of median CD8 expression on R v TF patients. Data are shown with box-whiskers graph, with bars indicating min to max. Data were compared using Mann-Whitney test. (**C-E**) Enriched donor NK cells (baseline) were assessed for CD8 and NKG2A. (**C**) Experimental Schema. (**D**) Representative plot showing frequency of $NKG2A^{+}CD8^{+}$ NK cells present in the baseline donor NK cells, inset numbers depict frequency of cells within the gate. (**E**) Summary from (**D**). (**F**) Freshly isolated NK cells were stimulated with IL-12/15/18 and phosphorylation of the indicated markers assessed at the indicated time points for $CD8^{+}$ and $CD8^{-}$ NK cells. Phosphorylation was induced in all markers ($p > 0.05$ for all conditions, one sample t test, test value = 1). No significant differences were observed between fold increases in phosphor-markers between the CD8 subsets, as determined by 2 way ANOVA. (**G-H**) $CD8^{-}$ and $CD8^{+}$ NK cells were

enriched from normal donor PBMC, labeled with CTV, and stimulated with IL-12/15/18 for 16 hours. (**G**) CTV dilution was measured by flow cytometry at day 7. Summary data were compared using a paired t test. (**H**) Intracellular Ki-67 was also assessed. Summary data were compared using a paired t test. (**I**) Median expression of Ki-67 on donor ML NK cells from TF and R patients at day 7, post-infusion. Data were compared using Mann-Whitney test. (**J**-**M**) CRISPR/Cas9 was utilized to delete CD8a from NK cells prior to 7-day ML NK differentiation. (**J**) Experimental schema. (**K**). Representative histogram of CD8α expression on WT or ΔCD8a ML NK cells. (**L**) K562 target killing by WT or ΔCD8a ML NK cells. (**M**) IFN-γ, TNF, and CD107 on WT and ΔCD8a ML NK cells stimulated with IL-12 + IL-15 or K562 tumor targets. Mean and SEM are depicted. Data from n = 4 normal donors from 2 independent experiments were compared using RM-ANOVA (L), and Paired t tests (M). P-values are indicated within the graphs.